2021 IEEE International Symposium on Safety, Security, and Rescue Robotics (SSRR)
New York, USA, October 25-27 2021

Flying-Climbing Mobile Robot for Steel Bridge Inspection

Anh Q. Pham, Anh T. La, Ethan Chang and Hung M. La, *IEEE Senior Member*

***Abstract*— The research of robots to assist people in inspecting the quality of steel bridges has attracted significant attention in recent years. However, the intricate structure of the steel bridge components poses a massive challenge for researchers to move the robot across the bridge to perform the tests. This paper presents a new development of a hybrid flying-climbing robotic system, which can move flexibly and quickly to different positions on the steel bridge. In addition to using high-resolution cameras for an overview, the design allows the robot to stick to steel surfaces and act as a mobile robot for more detailed inspection with our developed giant magneto-resistance (GMR) sensor array system. We conduct a mechanical analysis to show the climbing capability of the mobile part. Additionally, we develop a landing algorithm to allow the robot to land on a steel surface to perform in-depth inspection safely. The designed GMR sensor array has shown the capability of detecting steel cracks to support the in-depth inspection mode. We have tested and validated our developed robot on real bridges to ensure that the design works well and is stable.**

I. Introduction

Fig. 1: Dangerous bridge inspection scenes.

This work was funded by Vingroup Joint Stock Company and supported by Vingroup Innovation Foundation (VINIF) under project code VINIF.2020.NCUD.DA094, the U.S. National Science Foundation (NSF) under grants NSF-CAREER: 1846513 and NSF-PFI-TT: 1919127, and the U.S. Department of Transportation, Office of the Assistant Secretary for Research and Technology (USDOT/OST-R) under Grant No. 69A3551747126 through INSPIRE University Transportation Center, and the Japan NineSigma through the Penta-Ocean Construction Ltd. Co. under Agreement No. SP-1800087. The views, opinions, findings and conclusions reflected in this publication are solely those of the authors and do not represent the official policy or position of the VINIF, the NSF, the USDOT/OST-R and any other entities.

Anh Pham and Anh La are with the AIR-VIET Corporation, Vietnam. Ethan Chang and Hung La are with the Advanced Robotics and Automation (ARA) Lab, Department of Computer Science and Engineering, University of Nevada, Reno, NV 89557, USA. Corresponding author: Hung La, email: hla@unr.edu.

Fig. 2: The complexity of steel bridge structures.

Under the impact of the environment (such as wind, rain, sea steam, etc.) and the influence of overuse use leads to degradation of various structures on the steel bridge. Therefore, regular inspection and supervision are essential to ensure safe operation and help managers have timely assessment and maintenance to avoid unfortunate accidents.

Various types of robots have been created to assist humans in performing bridge testing instead of the dangerous and challenging manual methods (Fig. 1). Most designs act as a conventional mobile robot using circular wheels or tank wheels with direct magnets to create grip for the robot to move on steel surfaces [1]–[8].

In several other designs, researchers learned from the movement of animals, insects such as worms, and spiders for use in their designs. These designs show outstanding mobility as most of these designs can move back and forth between different surfaces on the steel bridge [9]–[12]. In the latest research, La's group [13], [14] has developed a robotic system that can climb various terrains on a steel bridge to perform the inspection. Their robot not only climbs like a worm but can also move around like a mobile robot.

With today's advanced image processing technology, the use of drones for visual inspection is becoming more and more common. Some developments to make aircraft move safely are presented in [17]–[19]. A drone design with passive rotating housings on each propeller for safer drone

2021 IEEE International Symposium on Safety, Security, and Rescue Robotics (SSRR) | 978-1-6654-1764-8/21/$31.00 ©2021 IEEE | DOI: 10.1109/SSRR53300.2021.9597676

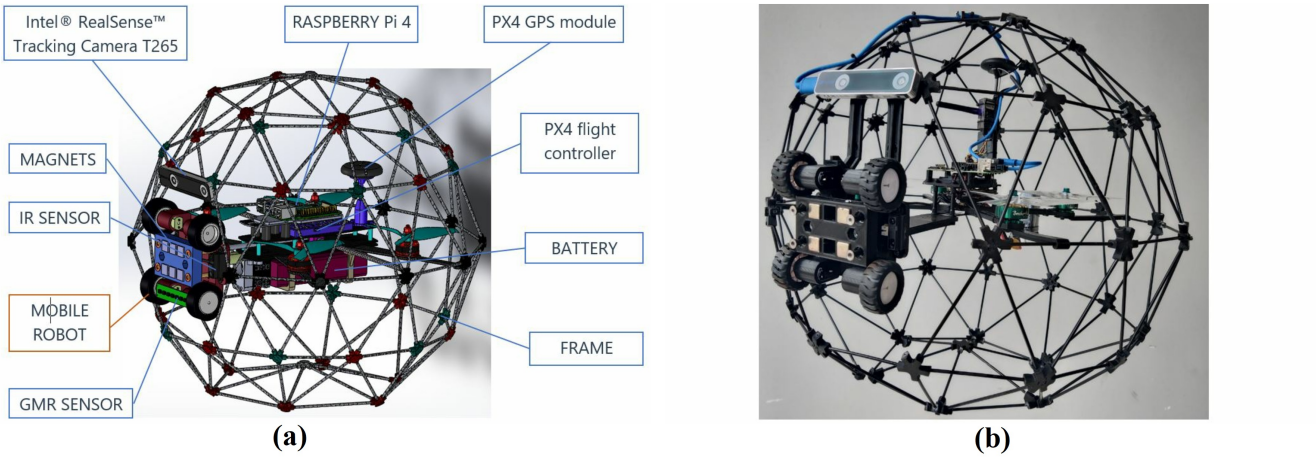

Fig. 3: (a) Overall design of robot, (b) Realistic robot.

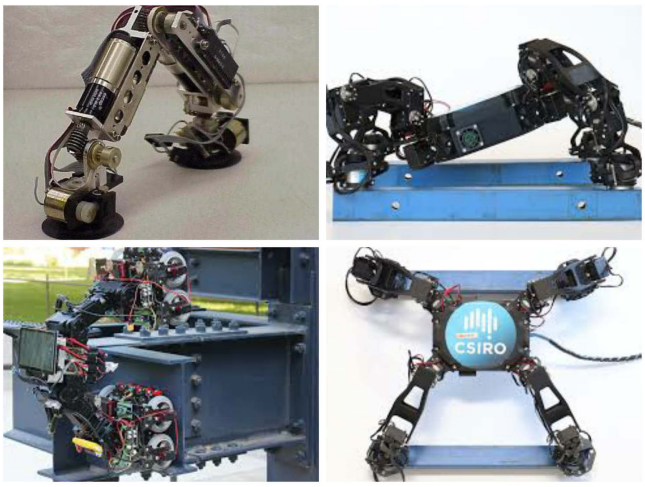

Fig. 4: Worm and Spider robot to inspect the bridge [13]–[16].

movement is presented in [20]. An improvement that saves flying energy [21] is the use of a clamp to hold the drone onto the bridge's beams for inspection.

In short, the mobile robot designs allow them to move stably on flat surfaces of the bridge. However, with the complex structure of the steel bridge as Fig. 2 switching between surfaces is also a significant challenge when using these types of design. Not to mention the performance of climbing on high-volume bridges will take a lot of time. Techniques for learning the way that animals and insects move (Fig. 4) have shown the feasibility of robots climbing over different connectors and surfaces on bridges [13]–[16]. However, each bridge has many locations to check, and they are usually not close together, so it will take a long time for those robots to complete the inspection of a bridge. Not to mention that calculation to move also takes a lot of time and requires intelligent algorithms. Studies on using drones for inspection allow a quick, efficient overview without being limited by structural steel or steel surfaces. However, the maintenance inspection of the steel requirement requires several positions that require in-depth tests that current drone studies have not yet applied.

Unlike the approaches mentioned above, this paper presents a new hybrid robotic design, which considers the advantages of a drone's flying flexibility and a mobile robot's steady climbing capability to perform quality inspection of steel bridges. With this design, the quality inspection of the steel bridge will be conducted faster, thanks to the drone's maneuverability. The mobile robot part of the design is equipped with permanent magnets that can change the distance from the steel surface. Changing the distance between the magnet and the steel surface allows the robot to switch its operating modes: landing, taking-off, moving. Giant magneto-resistance (GMR) sensor is fitted on the robot to serve for an in-depth inspection. The test results show that this sensor's ability to detect cracks is good. To demonstrate the robot's working principle, in addition to testing flight modes, testing for the robot to land on a steel surface was conducted.

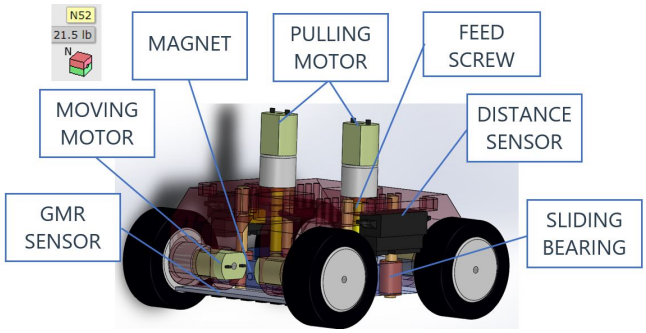

Fig. 5: Mobile robot part.

II. Overall Design

The design concept of this robot is illustrated in Fig. 3. The robot is divided into two main parts: mobile and drone.

The mobile part allows the robot to cling to steel surfaces and move like other conventional mobile robots (Fig. 5). On the robot, the body is attached to magnets to create attractive force when the robot clings to the steel surface. The distance between the magnet array and the steel face is controlled

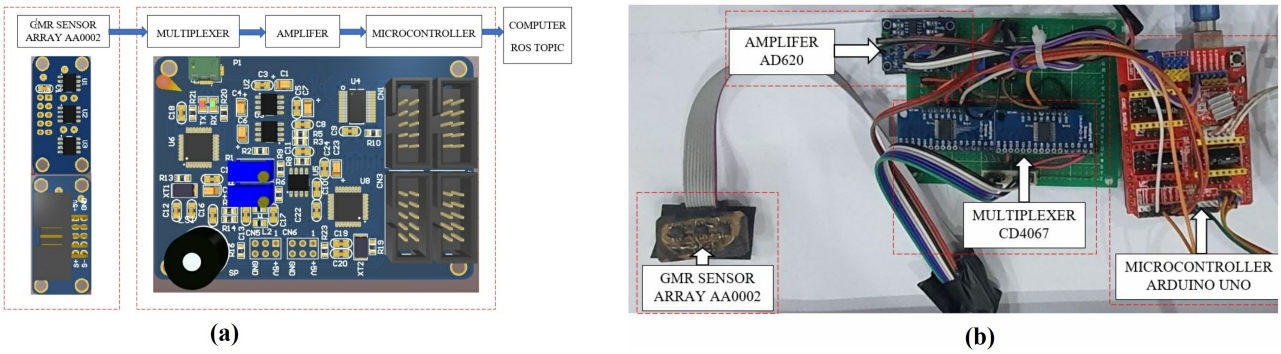

Fig. 6: (a) GMR sensor design, (b) Sample circuit for testing.

by two pull motors. This gap is divided into 3 cases: The robot clings to the steel surface to inspect as Fig. 7.a; the robot is in the moving state when the distance between the magnets and the steel surface is 2mm (Fig. 7.b; and when this distance reaches the limit of 20mm, the robot can take off to fly elsewhere as Fig. 7.c.)

Normally the robot will operate in drone mode. In this mode, the robot uses a high-resolution camera to capture images of the surface of the steel bars, the joint positions on the bridge. At the same time, send photos to investigators for live viewing. When potential damage is detected that needs more in-depth investigation, the mobile part will change from Fig. 7.d to Fig. 7.e, available sieve to adhere to the steel surface. It then relies on the values of 2 proximity sensors along with an intelligent algorithm to determine if the point in front is a safe position to land (Fig. 7.a.b.c).

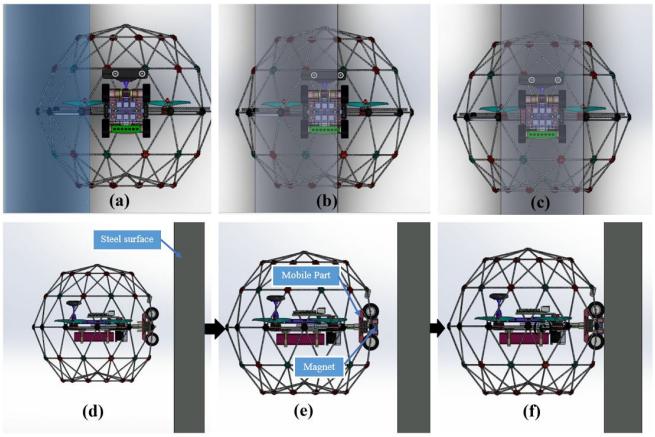

Fig. 7: (a) The robot has completely deviated from the steel surface; (b) The robot is deflected to one side of the steel surface; (c) The robot is safe to land on a steel surface; (d, e, f) When the motion robot attaches to the steel surface.

In addition to building a robotic design that combines the drone and mobile robot, we designed an GMR sensor circuit using NVE AA002 for the robot to perform more thorough steel crack tests. In studies [22]–[25], GMR sensors are considered to have been used to check for defects by quickly scanning an area and generating high-resolution test results. Our designed sensor system diagram is shown in Fig. 6, and installed for testing as shown in Fig. 8. The steel sample we examine here has a thickness of 6 mm, and the artificial cracks are 0.1 mm, 0.2 mm, 0.3 mm, and 0.5 mm, respectively. The use of rails will allow for a stabler test than when we move the sensor by hand.

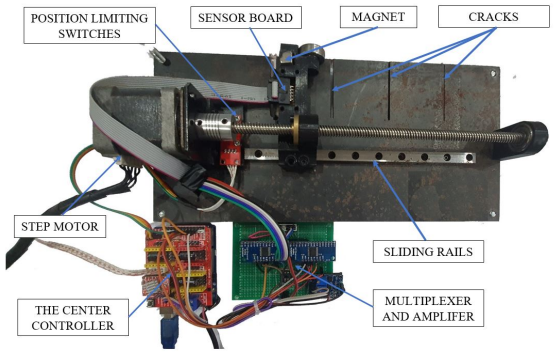

Fig. 8: Structure test of the ability to check the GMR sensor for crack detection.

III. Mechanical Design and Analysis

We used the following type of motor for the drone: Brother-Hobby LPD 2806.5, motor: 1300KV, configuration: 12N14P, No.of Cells (Lipo): 4-6S, rotor: N52H arc magnets, copper wire: 260°C military grade, stator: 0.2mm Kawasaki silicon steel, shaft: titanium alloy hollow shaft, bearings: Japanese NMB 12X6X4, wire AWG: 18AWG 20cm length, bell cap: Al 7075, base casing: Al 7075, prop adapter shaft thread: M5, bolt pattern: M3 (19X19mm). Fig. 9 presents the test data of the drone motor's load.

We used the following type of motor for the mobile robot: motor DC GA20Y130, voltage operating range: 3-9 VDC, load speed 90 RPM, load current 0.07A, torque 0.31 N.m.

We conducted a series of static analyses on the robot throughout the design process. These tests allowed us to design and manufacture robots that outperformed previous designs of other steel bridge test robots such as [26], [27].

1300KV Test data								
Item No.	Prop (inch)	Throttle (%)	Valtage (V)	Current (A)	RPM	Thrust (gf)	Input Power (W)	Thrust efficiency (G/W)
2806.5BN 1300KV	HQ7.0*3.5*3	30	24.0	2.3	8270	310	55.20	5.62
		40	24.0	4.6	10517	530	110.40	4.80
		50	24.0	7.2	12132	750	172.80	4.34
		60	24.0	12.7	14922	1130	304.80	3.71
		70	23.9	18.3	16785	1430	437.37	3.27
		80	23.9	28.8	19216	1940	688.32	2.82
		90	23.8	37.5	20631	2290	892.50	2.57
		100	23.8	44.4	21691	2520	1056.72	2.38
The temperature of inside copper wire is 102.2℃ after 100% throttle running 2 mins. (Ambient temperature is 28℃)								

Fig. 9: Drone motor's load test data.

Magnetic grip analysis ensures that we make the right choice of materials, preventing the robot from tipping over or slipping during operation.

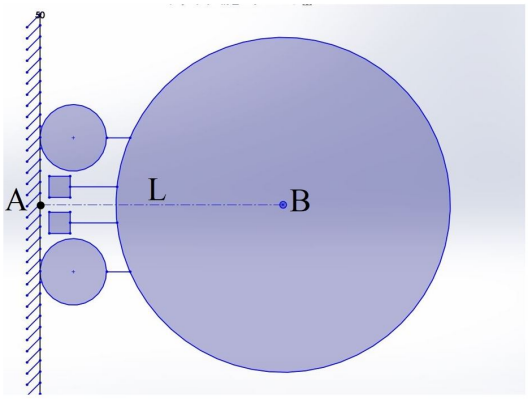

Fig. 10: Extended statics diagram.

The variable L is the distance from the robot's center to the outside of the wheel, which is the distance from point A to point B as shown in Fig. 10. m is the mass of the robot, and g is the gravity. The moment at point A is calculated by the formula:

$$M_A = Lmg. \tag{1}$$

Through Equ. (1), where g is constant, we find that the mass m plays a large role in the corresponding effect. That is why we decided to use carbon and plastic as the main materials instead of conventional metal materials. This significantly reduces the robot's mass (reduces the moment to override the gravity).

The ability to flip and slip while operating the robot is entirely possible, so we conducted two additional analyses to clarify them in our design.

Our flip analysis (Fig. 11.a) uses Equ. (1) as an action that can flip the robot. To calculate how much suction power is required for the mobile part to prevent tipping, at point C creates the Equ. (2). The variables $n1$, $n2$ represent the number of magnets in each row. M_C is the Moment at point C, F_{mag} is the force created by each magnet, and L_1, L_2 all represent distances.

$$M_C = F_{mag}n_1L_2 + F_{mag}n_2(L_1 + L_2) - M_A. \tag{2}$$

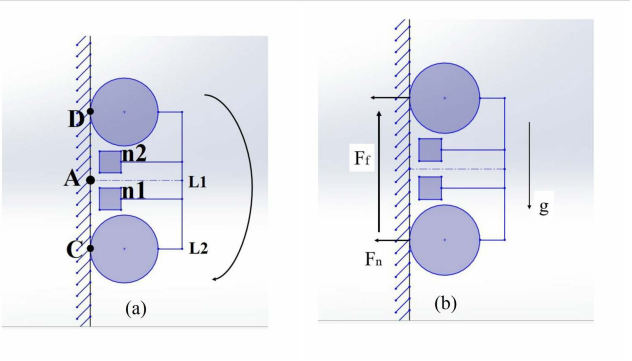

Fig. 11: (a) Turn-over diagram, (b) adhesion diagram.

Results of Equ. (2) will help in choosing the strength of the magnet and the mounting position to ensure that the robot will maintain its position on steel structures without tipping.

Analysis of sliding friction (Fig. 11.b) to ensure that the robot does not slip down when clinging to the steel surface is necessary. The friction force is calculated by:

$$F_f = nF_{mag}\mu, \tag{3}$$

where, F_f is the friction force, F_{mag} is the force generated by one magnet, n is the total number of permanent magnets, and μ represents the friction coefficient between steel and rubber.

Equ. (2) and Equ. (3) help us choose the right magnet to use for robot design.

IV. Tele-operation

Controlling the robot at a long distance will be difficult, requiring the operator to have enough vision and a good feeling. Solution using VR glasses to view images directly from the robot allows the operator to have a better view instead of watching from afar. A camera is connected and transmits the image to the VR headset at 5.8 GHz, the equipment is shown in Fig. 12. In addition, the protective frame helps the robot avoid unfortunate collisions.

Fig. 12: The VR system.

Despite obtaining good visibility through the VR glasses, determining the distance to landing on a steel surface is relatively difficult. We have equipped two more proximity sensors on both sides of the robot's mobile part (Fig. 5), combined with Algorithm 1 to perform the automatic landing. Where IR_l and IR_r are the values of the two proximity sensors on left and right sides of the robot, respectively. IR_{le} and IR_{re} are values when the two sensors do not detect

Algorithm 1: LANDING ON A STEEL SURFACE.

Input: (IR_l, IR_r),(IR_{le}, IR_{re}),(IR_{ld}, IR_{rd}),(IR_{ll}, IR_{rl})

```
while robot is landing do
    Read sensor value
    if (IR_l) ==(IR_ll) and (IR_r) ==(IR_rl) then
        STOP.
        Break to manual mode.
    if (IR_l) ==(IR_le) and (IR_r) ==(IR_re) then
        Stop landing and hold the position.
        Send warnings to the operator.
        Break to manual mode.
    else
        if (IR_l) ==(IR_ld) then
            if (IR_r) ==(IR_re) then
                Move right
                while (IR_r) ==(IR_re) do
                    Wait until (IR_r) =(IR_rd).
                    Move forward.
                Move forward.
            else
                Move forward.
        else
            if (IR_r) ==(IR_re) then
                if (IR_l) ==(IR_le) then
                    Move left.
                    while (IR_l) ==(IR_le) do
                        Wait until (IR_l) =(IR_ld).
                        Move left.
                    Move forward.
                else
                    Move forward.
```

the front obstacle. IR_{ld} and IR_{rd} are the values when two sensors detect the front obstacle (steel frame). IR_{ll} and IR_{rl} are the values of the two sensors when the robot lands.

V. ROBOT DEPLOYMENT

The result of the designed GMR sensor array system's ability to detect the crack is shown in Fig. 13. The GMR sensor's signal value in cracked areas is significantly higher than the ones in non-cracked areas. The width of the cracks was inferred from the lifetime of the abnormally high pulse signals measured from the time the crack was detected until its termination. As shown in Fig. 13 that is the value of Ts. With this result, it can be confirmed that attaching sensors to the robot for inspection is entirely possible.

The testing of changing the distance between the magnet surface and the steel surface has been conducted many times by the team to ensure that the robot can push the magnet away, thereby being ready for landing and clinging to the surface steel or pulling the magnet back to get ready for easy takeoff. In addition, the test of the safe location function

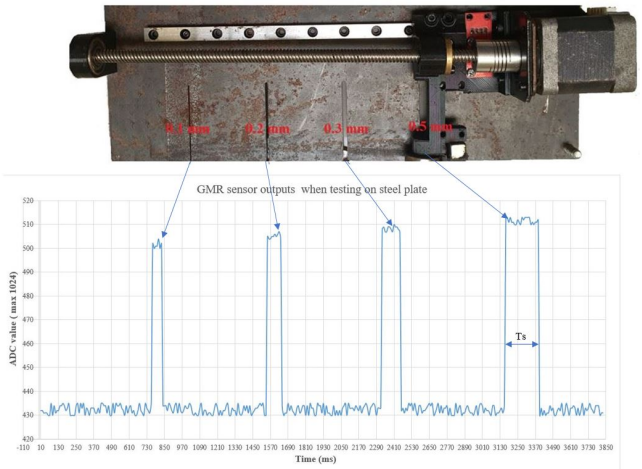

Fig. 13: GMR sensor test results of crack detection.

is also conducted carefully to ensure that the robot, when testing in a real environment, is safe.

The authors have conducted an experiment at the Nam-O bridge in Da Nang City, Vietnam. This is a steel bridge for trains, located near the sea, so the wind here is strong. However, the team found that the robot can move flexibly and cling to the steel surface to observe and examine defects at a few critical points through the tests. Some pictures of rusted screws that need replacement on the Nam O bridge were taken as shown in Fig. 15.

During the field deployment, the robot can work continuously for 30 minutes with the current setting of two 22.2V, 13000mAh LiPo batteries.

Fig. 14: Robot test on the Nam-O bridge.

VI. CONCLUSION AND FUTURE WORK

The hybrid flying-climbing robot described in this paper presented a new design that utilizes the advantages of the drone's flying flexibility and the mobile robot's steady climbing capability to perform an inspection of complex steel structures of the bridge. The robot can switch from flying to climbing for quick back and forth in multiple locations on the bridge and perform both visual inspection (using camera) and in-depth inspection (using our developed GMR sensor

Fig. 15: Some pictures on the Nam-O bridge.

array), thanks to the drone's maneuverability and the ability to land on steel surface. The mechanical design and analysis have been conducted to show the climbing capability of the mobile part. The landing algorithm has been developed to allow the robot to land on a steel surface to perform in-depth inspection safely. The designed GMR sensor array has shown the capability of detecting steel cracks to support the in-depth inspection mode of the robot. The proposed hybrid design has been tested and validated on real bridges to ensure that the design works well and is stable.

Equipping the GMR sensor array under the mobile body of the robot demonstrates the ability of a lightweight sensor to check for steel cracks. However, with the current installation, there will be some corner areas of the bridge that may not be reached to inspect with this GMR sensor array but can only be checked via camera. Therefore in the future, we will design an additional arm equipped with this GMR sensor so that the robot can check in more difficult-to-reach areas.

REFERENCES

[1] W. Shen, J. Gu, and Y. Shen, "Permanent magnetic system design for the wall-climbing robot," in *IEEE Intern. Conf. Mechatronics and Automation, 2005*, vol. 4. IEEE, 2005, pp. 2078–2083.

[2] A. Q. Pham, H. M. La, K. T. La, and M. T. Nguyen, "A magnetic wheeled robot for steel bridge inspection," in *Intern. Conf. on Engineering Research and Applications*. Springer, 2019, pp. 11–17.

[3] H. M. La, T. H. Dinh, N. H. Pham, Q. P. Ha, and A. Q. Pham, "Automated robotic monitoring and inspection of steel structures and bridges," *Robotica*, vol. 37, no. 5, pp. 947–967, 2019.

[4] S. T. Nguyen and H. M. La, "Roller chain-like robot for steel bridge inspection," *The 9th Intern. Conf. on Structural Health Monitoring of Intelligent Infrastructure (SHMII-9)*, 2019.

[5] D. Zhu, J. Guo, C. Cho, Y. Wang, and K.-M. Lee, "Wireless mobile sensor network for the system identification of a space frame bridge," *IEEE/ASME Trans. On Mechatronics*, vol. 17, no. 3, pp. 499–507, 2012.

[6] G. Lee, G. Wu, J. Kim, and T. Seo, "High-payload climbing and transitioning by compliant locomotion with magnetic adhesion," *Robotics and Autonomous Systems*, vol. 60, no. 10, pp. 1308–1316, 2012.

[7] J. Guo, W. Liu, and K.-M. Lee, "Design of flexonic mobile node using 3d compliant beam for smooth manipulation and structural obstacle avoidance," in *2014 IEEE Intern. Conf. on Robotics and Automation (ICRA)*. IEEE, 2014, pp. 5127–5132.

[8] S. T. Nguyen and H. M. La, "A climbing robot for steel bridge inspection," *Journal of Intelligent Robotic Systems*, vol. 102, no. 4, pp. 1–21, 2021.

[9] A. Lopez-Lora, P. Sanchez-Cuevas, A. Suarez, A. Garofano-Soldado, A. Ollero, and G. Heredia, "Mhyro: Modular hybrid robot for contact inspection and maintenance in oil amp; gas plants," in *2020 IEEE/RSJ Intern. Conf. on Intelligent Robots and Systems (IROS)*, 2020, pp. 1268–1275.

[10] T. Bandyopadhyay, R. Steindl, F. Talbot, N. Kottege, R. Dungavell, B. Wood, J. Barker, K. Hoehn, and A. Elfes, "Magneto: A versatile multi-limbed inspection robot," in *2018 IEEE/RSJ Intern. Conf. on Intelligent Robots and Systems (IROS)*. IEEE, 2018, pp. 2253–2260.

[11] A. Mazumdar and H. H. Asada, "Mag-foot: A steel bridge inspection robot," in *2009 IEEE/RSJ Intern. Conf. on Intelligent Robots and Systems*. IEEE, 2009, pp. 1691–1696.

[12] P. Ward, P. Manamperi, P. Brooks, P. Mann, W. Kaluarachchi, L. Matkovic, G. Paul, C. Yang, P. Quin, D. Pagano *et al.*, "Climbing robot for steel bridge inspection: Design challenges," in *Austroads Bridge Conf.* ARRB Group, 2014.

[13] S. T. Nguyen, A. Q. Pham, C. Motley, and H. M. La, "A practical climbing robot for steel bridge inspection," in *2020 IEEE Intern. Conf. on Robotics and Automation (ICRA)*. IEEE, 2020, pp. 9322–9328.

[14] H.-D. Bui, S. Nguyen, U. Billah, C. Le, A. Tavakkoli, and H. M. La, "Control framework for a hybrid-steel bridge inspection robot," in *2020 IEEE/RSJ Intern. Conf. on Intelligent Robots and Systems (IROS)*. IEEE, 2020, pp. 2585–2591.

[15] B. Tirthankar, S. Ryan, T. Fletcher, K. Navinda, D. Ross, W. Brett, B. James, H. Karsten, and E. Alberto, "Magneto: A versatile multi-limbed inspection robot," in *Proceedings of the 2018 IEEE/RSJ Intern. Conf. on Intelligent Robots and Systems (IROS), Madrid, Spain*, 2018, pp. 1–5.

[16] M. Minor, H. Dulimarta, G. Danghi, R. Mukherjee, R. L. Tummala, and D. Aslam, "Design, implementation, and evaluation of an under-actuated miniature biped climbing robot," in *Proceedings. 2000 IEEE/RSJ Intern. Conf. on Intelligent Robots and Systems (IROS 2000)(Cat. No. 00CH37113)*, vol. 3. IEEE, 2000, pp. 1999–2005.

[17] N. Meiri and D. Zarrouk, "Flying star, a hybrid crawling and flying sprawl tuned robot," in *2019 Intern. Conf. on Robotics and Automation (ICRA)*, 2019, pp. 5302–5308.

[18] Flyability, "Elios 2," https://www.youtube.com/watch?v=hW1Fn32JBls%2F., Dec. 2020.

[19] C. study, "Advancing bridge inspections with intel's drone solutions," https://www.intel.com/content/www/us/en/products/docs/drones/advancing-bridge-inspections-case-study.html, Dec. 2020.

[20] C. J. Salaan, K. Tadakuma, Y. Okada, Y. Sakai, K. Ohno, and S. Tadokoro, "Development and experimental validation of aerial vehicle with passive rotating shell on each rotor," *IEEE Robotics and Automation Letters*, vol. 4, no. 3, pp. 2568–2575, 2019.

[21] "Birds," https://inspire-utc.mst.edu/researchprojects/as-4/, Dec. 2020.

[22] A. Yashan, W. Bisle, and T. Meier, "Inspection of hidden defects in metal-metal joints of aircraft structures using eddy current technique with gmr sensor array," *Proc. 9th ECNDT, Berlin*, 2006.

[23] O. Postolache, A. L. Ribeiro, and H. G. Ramos, "Gmr array uniform eddy current probe for defect detection in conductive specimens," *Measurement*, vol. 46, no. 10, pp. 4369–4378, 2013.

[24] N. Gloria, M. Areiza, I. Miranda, and J. Rebello, "Development of a magnetic sensor for detection and sizing of internal pipeline corrosion defects," *NDT & E Inter.*, vol. 42, no. 8, pp. 669–677, 2009.

[25] M. M. Tehranchi, M. Ranjbaran, and H. Eftekhari, "Double core giant magneto-impedance sensors for the inspection of magnetic flux leakage from metal surface cracks," *Sensors and Actuators A: Physical*, vol. 170, no. 1-2, pp. 55–61, 2011.

[26] P. Ward, P. Manamperi, P. Brooks, P. Mann, W. Kaluarachchi, L. Matkovic, G. Paul, C. Yang, P. Quin, D. Pagano *et al.*, "Climbing robot for steel bridge inspection: Design challenges," in *Austroads Bridge Conf.* ARRB Group, 2014.

[27] M. Eich and T. Vögele, "Design and control of a lightweight magnetic climbing robot for vessel inspection," in *2011 19th Mediterranean Conf. on Control & Automation (MED)*. IEEE, 2011, pp. 1200–1205.